Temperature−Composition Phase Diagrams for Binary Blends Consisting of Chemically Dissimilar Diblock Copolymers

Nitin Y. Vaidya and Chang Dae Han*

Department of Polymer Engineering, The University of Akron, Akron, Ohio 44325-0301

Received November 5, 1999

ABSTRACT: Temperature−composition phase diagrams for binary blends of chemically dissimilar diblock copolymers, (A-*block*-B) and (A-*block*-C) copolymers, were constructed experimentally. For the study, two polystyrene-*block*-polyisoprene (SI diblock) copolymers (SI-7/8 and SI-10/53) and three polystyrene-*block*-polybutadiene (SB diblock) copolymers (SB-9/8, SB-5/36, and SB-10/10) were used. Three binary blend systems were prepared: (i) (SI-7/8)/(SB-9/8) blends consisting of two nearly *symmetric* lamella-forming diblock copolymers having different chemical structures, (ii) (SI-10/53)/(SB-5/36) blends consisting of two highly *asymmetric* sphere-forming diblock copolymers having different chemical structures, and (iii) (SB-10/10)/(SB-9/8) blends consisting of two nearly *symmetric* lamella-forming diblock copolymers having different microstructures in the polybutene block. It has been found, via transmission electron microscopy (TEM), that *no* macrophase separation took place in each binary blend system over the entire range of blend compositions investigated. The order−disorder transition temperature of each binary blend was determined using oscillatory shear rheometry, enabling us to construct a temperature−composition phase diagram for each blend system. It has been found that the temperature−composition phase diagrams for the (SB-9/8)/(SI-7/8) and (SB-10/10)/(SB-9/8) blend systems follow nearly a linear relationship, whereas the temperature−composition phase diagrams for the (SI-10/53)/(SB-5/36) blend system show positive deviation from linearity. The experimentally determined temperature−composition phase diagrams are found to be consistent with the predictions from random phase approximation calculations. It has been found that the microdomain structure, as determined by TEM, of each binary blend was the same as that of the constituent block copolymers.

Introduction

Binary blends of block copolymers offer a unique opportunity to produce a new class of polymeric materials in that one has a great deal of flexibility in the choice of constituent components.[1] In the past, a large number of experimental[2−21] and theoretical[22−29] investigations were reported on various issues (e.g., morphology, phase separation, phase transition) associated with the binary blends of diblock copolymers. With a few exceptions,[2−4] most of the experimental[5−21] and theoretical studies[22−29] reported so far have dealt with (A-*block*-B)$_1$/(A-*block*-B)$_2$ blends having identical chemical structure, but different molecular weights or different block length ratios. Using (A-*block*-B)$_1$/(A-*block*-B)$_2$ blends, some research groups[5−13] investigated ordered structure, others[14,15] investigated copolymer block distributions within the domains and interfacial profiles, and still others[16−20] investigated order−order or order−disorder phase transitions. Only a few research groups[16−18] reported on temperature−composition phase diagrams of the (A-*block*-B)$_1$/(A-*block*-B)$_2$ blends.

Binary blends of microphase-separated diblock copolymers can give rise to very complex morphology, because they may undergo both micro- and macrophase separations, depending upon the molecular parameters of the constituent blocks and the extent of miscibility (or repulsive interactions) between the constituent blocks.[3−7] For instance, in the (A-*block*-B)$_1$/(A-*block*-B)$_2$ blends there are six independent variables: (i) the lengths of each of the blocks forming the two copolymers (four variables), (ii) the interaction parameter between A and B segments (one variable), and (iii) the volume fraction of the blend (one variable). Other factors that would also affect the phase behavior of the (A-*block*-B)$_1$/(A-*block*-B)$_2$ blends are (i) the ratio of overall molecular weights of the two diblock copolymers, $M_{C,1}/M_{C,2}$, (ii) the difference in the volume fraction of block A in the respective diblock copolymers, $(f_{A,1} - f_{A,2})$, and (iii) the volume fraction of a constituent diblock copolymer in the blend, $\phi_{C,1}$, or the overall volume fraction of block A in the binary blend, ϕ_A^T. On the other hand, in the (A-*block*-B)/(C-*block*-D) blends consisting of two *chemically dissimilar* diblock copolymers, there are 11 independent variables: (i) 6 pairs of the interaction parameters, (ii) block length of each of the 4 chemically different blocks in the two copolymers (4 variables), and (iii) the volume fraction of the blend (1 variable). It is then obvious that (A-*block*-B)/(A-*block*-C) and (A-*block*-B)$_1$/(A-*block*-B)$_2$ blends can be regarded as being special cases of the most general (A-*block*-B)/(C-*block*-D) blends.

On the theoretical side, Shi and Noolandi[24] used self-consistent mean-field theory to investigate the phase behavior of (A-*block*-B)$_1$/(A-*block*-B)$_2$ blends. They showed that small amounts of short diblock copolymer chains at the interfaces may shift the phase boundaries of the system, suggesting that the morphologies of long diblock copolymer can be modified by the addition of short diblock chains. However, their theory is applicable to the situations where the blocks of the short diblock copolymer are not too large and the concentration of the short diblock is low enough, such that micelle formation can be ignored. Shi and Noolandi[25] constructed *isothermal* phase diagrams for a (A-*block*-B)$_1$/(A-*block*-B)$_2$ blend system having the same degree of polymerization, $Z_{C,1} = Z_{C,2}$, but different values of $f_{A,1}$, $f_{A,2}$, and $\phi_{C,1}$ in the blends. Without restriction to strong segregation regime, using self-consistent mean-field theory, Matsen[28] constructed phase diagrams for the (A-*block*-B)$_1$/(A-*block*-B)$_2$ blends in which both block copolymers have *lamellar* microdomains. He predicted that the lamella-forming

10.1021/ma9918755 CCC: $19.00
Published on Web 03/18/2000

(A-*block*-B)$_1$/(A-*block*-B)$_2$ blends having $Z_{C,1}/Z_{C,2} > 5$ may phase separate into two distinct lamellar phases or coexist in the lamellar and disordered phases. We are not aware of any theoretical study reported on temperature−composition phase diagrams for the (A-*block*-B)/(A-*block*-C) or (A-*block*-B)/(C-*block*-D) blends.

Very recently, we investigated experimentally the phase transition in (A-*block*-B)/(A-*block*-C) blends and constructed temperature−composition phase diagrams of the blend system. For the study, we employed two polystyrene-*block*-polyisoprene (SI diblock) copolymers and three polystyrene-*block*-polybutadiene (SB diblock) copolymers. Both SI diblock copolymers had 94% 1,4-addition in polyisoprene (PI) block, but one of the SI diblock copolymers (SI-10/53) had spherical microdomains of polystyrene (PS) while the other SI diblock copolymer (SI-7/8) had lamellar microdomains with alternating layers of PS and PI. One of the three SB diblock copolymers (SB-10/10) had 91% 1,4-addition in polybutadiene (PB) block and lamellar microdomains, the second SB diblock copolymer (SB-9/8) had 89% 1,2-addition in PB block and lamellar microdomains, and the third SB diblock copolymer (SB-5/36) had 86% 1,2-addition in PB block and spherical microdomains of PS. Using these five diblock copolymers, we prepared three binary blend systems: (i) (PS-*block*-1,4-PI)/(PS-*block*-1,2-PB) blends with lamella-forming constituent copolymers, (ii) (PS-*block*-1,4-PI)/(PS-*block*-1,2-PB) blends with sphere-forming constituent copolymers, and (iii) (PS-*block*-1,2-PB)/(PS-*block*-1,4-PB) blends with lamella-forming constituent copolymers. It should be mentioned that a pair of 1,4-PI and 1,2-PB have attractive segment−segment interactions[30] and thus blends of 1,4-PI and 1,2-PB are miscible, whereas a pair of 1,2-PB and 1,4-PB have repulsive segment−segment interactions[31] and thus blends of 1,2-PB and 1,4-PB are immiscible. We found, via transmission electron microscopy (TEM), no evidence of macrophase separation in each of the three blend systems over the entire range of blend compositions investigated. Using oscillatory shear rheometry, we determined the order−disorder transition (ODT) temperature (T_{ODT}) of each binary blend. In the absence of macrophase separation, we were able to construct temperature−composition phase diagram with information on the T_{ODT} of each binary blend. Using TEM, we also investigated the microdomain structures of the binary blends. In this paper, we report the highlights of our findings.

Experimental Section

Materials. Two SI diblock copolymers (SI-7/8 and SI-10/53) were synthesized via anionic polymerization in our laboratory. Two SB diblock copolymers (SB-9/8 and SB-5/36) were supplied to us by Dr. Adel F. Halasa of Goodyear Tire and Rubber Company, and one SB diblock copolymer (SB-10/10) was supplied to us by Dr. Steve F. Hahn of Dow Chemical Company. Nuclear magnetic resonance spectroscopic analyses indicate the following: (i) PI block in SI-7/8 and SI-10/53 has 94% 1,4-addition, 6% 3,4-addition and no detectable amount of 1,2-addition, (ii) PB block in SB-9/8 and SB-5/39 has a very high vinyl content (ca. 90%), and (ii) PB block in SB-10/10 has a very low vinyl content (9%). Table 1 gives a summary of the molecular characteristics of these block copolymers. In this study, we chose the following three binary blend systems: (i) (SI-7/8)/(SB-9/8), (ii) (SB-10/10)/(SB-9/8), and (iii) (SI-10/53)/(SB-5/36) blends. The special features of each blend system chosen in this study are summarized in Table 2. It is worth noting that each blend system selected in this study consists of two *chemically dissimilar* diblock copolymers, which then must be viewed as (A-*block*-B)/(A-*block*-C) blends.

Table 1. Molecular Characteristics of the Diblock Copolymers Investigated in This Study

sample code	M_n (g/mol)	M_w/M_n	w_{PS}[a]	f_{PS}[b]	Z_C[c]
SI-7/8[d]	1.44×10^4	1.02	0.48	0.43	179
SI-10/53[d]	5.67×10^4	1.12	0.16	0.15	879
SB-9/8[e]	1.67×10^4	1.04	0.53	0.48	240
SB-10/10[f]	1.91×10^4	1.06	0.50	0.45	284
SB-5/36[g]	4.08×10^4	1.02	0.13	0.11	721

[a] w_{PS} is the weight fraction of PS in the diblock copolymer. [b] f_{PS} is the volume fraction of PS in the diblock copolymer at 25 °C. [c] Degree of polymerization defined by $Z_C = M_{w,PS}/104.14 + M_{w,PI}/68.11$ for the SI diblock copolymer and $Z_C = M_{w,PS}/104.14 + M_{w,PB}/54.09$ for the SB diblock copolymer. [d] PI block contains 94% 1,4-addition. [e] PB block contains 89% 1,2-addition. [f] PB block contains 91% 1,4-addition. [g] PB block contains 86% 1,2-addition.

Sample Preparation. Samples were prepared by first dissolving a predetermined amount of neat block copolymer or a binary blend of block copolymers in toluene in the presence of 0.1 wt % antioxidant (Irganox 1010, Ciba-Geigy Group) and then slowly evaporating the solvent. The evaporation of toluene was carried out initially in a fume hood at room temperature for a week and then in a vacuum oven at 40 °C for 3 days. The last trace of toluene was removed by drying the samples in a vacuum oven at elevated temperature by gradually raising the oven temperature to 10 °C above the glass-transition temperature (T_g) of the PS phase in each block copolymer. The drying of the samples was continued until there was no further change in weight. Specimens for rheological measurements were annealed further, the details of which will be given in the figure captions.

Rheological Measurement. In this study, a Rheometrics mechanical spectrometer (model RMS 800) was used in the oscillatory mode with parallel plate fixtures (25 mm diameter). Dynamic frequency sweep experiments were conducted, i.e., the dynamic storage (G') and dynamic loss moduli (G'') were measured as functions of angular frequency (ω) ranging from 0.01 to 100 rad/s at various temperatures during heating. The temperature increment in the frequency sweep experiment varied from 3 to 10 °C, and the specimen was kept at a constant temperature for 30−40 min before rheological measurements actually began. Data acquisition was accomplished with the aid of a microcomputer interfaced with the rheometer. The temperature control was satisfactory to within ±1 °C. For the rheological measurements, the strain was varied from 0.03% to 0.3%, depending upon the measurement temperature, which was well within the linear viscoelastic range for the materials investigated. Dynamic temperature sweep experiments under isochronal conditions were also conducted, i.e., G' and G'' were measured at $\omega = 0.01$ rad/s during heating. All experiments were conducted under a nitrogen atmosphere in order to preclude oxidative degradation of the samples.

Transmission Electron Microscopy. TEM was conducted to investigate the morphology of the neat block copolymers and their binary blends. The ultrathin sectioning was performed by cryoultramicrotomy at −100 °C using a diamond knife, which was below the glass-transition temperature ($T_g = -68$ °C) of PI and below the T_g (=−98 °C) of PB, to attain the rigidity of the specimen, using a Richert Ultracut S low-temperature sectioning system. A transmission electron microscope (JEM1200EX II, JEOL) operated at 120 kV was used to record the morphology of the specimens stained with osmium tetroxide vapor.

Differential Scanning Calorimetry (DSC). T_g's of selected blend specimens were determined using DSC. DSC measurements were conducted on a Perkin-Elmer DSC-7 equipped with an ice−water cooling system, under a nitrogen atmosphere, at a heating rate of 20 °C/min. Sample size used was 10−15 mg. Indium was used to calibrate the DSC cell constant.

Table 2. Special Features of the Binary Mixtures of Diblock Copolymers Investigated in This Study[a]

sample code	$\lvert w_{PS,1} - w_{PS,2} \rvert$	$M_{C,1}/M_{C,2}$	$Z_{C,1}/Z_{C,2}$	special features
(SB-9/8)/(SI-7/8) blends	0.05	1.18	1.33	nearly symmetric diblock copolymers having different chemical structures
(SI-10/53)/(SB-5/36) blends	0.04	1.53	1.22	highly asymmetric diblock copolymers having different chemical structures
(SB-10/10)/(SB-9/8) blends	0.03	1.16	1.18	nearly symmetric diblock with a large difference in the microstructure of PB block

[a] $w_{PS,1}$ and $w_{PS,2}$ denote the weight fractions of PS in block copolymer 1 and in block copolymer 2, respectively. $M_{C,1}/M_{C,2}$ denotes the ratio of the molecular weight of block copolymer 1 and the molecular weight of block copolymer 2. $Z_{C,1}/Z_{C,2}$ denotes the ratio of the degree of polymerization of block copolymer 1 and the degree of polymerization of block copolymer 2.

Table 3. Summary of the T_{ODT}'s Determined from Han Plot for the Diblock Copolymers Investigated in This Study

sample code	chemical structure	microstructure	w_{PS}[a]	Z_C[b]
SI-7/8	PS-*block*-PI	94% 1,4-addition in PI block	0.43	179
SI-10/53	PS-*block*-PI	94% 1,4-addition in PI block	0.15	879
SB-9/8	PS-*block*-PB	89% 1,2-addition in PB block	0.48	240
SB-10/10	PS-*block*-PB	91% 1,4-addition in PB block	0.45	284
SB-5/36	PS-*block*-PB	86% 1,2-addition in PB block	0.11	721

[a] Weight fraction of PS in the block copolymer. [b] Degree of polymerization.

Results and Discussion

According to the literature,[3−7] a blend of two block copolymers may undergo both micro- and macrophase separations, depending upon the solubility of the two block copolymers, which in turn depends on the molecular weights of the constituent copolymers. In the present study, using TEM we first investigated whether macrophase separation occurred in each binary system chosen (see Table 2) and found that *no* macrophase separation occurred over the entire range of blend compositions investigated. Therefore, our task in the present study was much simplified in that we only had to determine the temperature (i.e., T_{ODT}) at which a pair of diblock copolymers undergo microphase separation, to construct the temperature−composition phase diagram. Below, we will first describe briefly the experimental procedure employed to determine T_{ODT} and then the temperature−composition phase diagram of each binary system investigated in this study.

Phase Diagram for the (SB-9/8)/(SI-7/8) Blend System. The rationale behind the selection of this blend system lies in that both SB-9/8 and SI-7/8 are nearly symmetric in composition but have different chemical structures. As summarized in Table 3, SB-9/8 contains 89% 1,2-addition in PB block, and SI-7/8 contains 94% 1,4-addition in PI block. Thus, for the sake of our discussion below, we will assume that SB-9/8 is very close to a PS-*block*-1,2-PB copolymer and that SI-7/8 is very close to a PS-*block*-1,4-PI copolymer. Thus, (SB-9/8)/(SI-7/8) blends represent (A-*block*-B)/(A-*block*-C) blends.

Figure 1 gives the temperature dependence of G' from the isochronal dynamic temperature sweep experiments at $\omega = 0.01$ rad/s for various (SB-9/8)/(SI-7/8) blends. In the literature,[32] it has been suggested that the T_{ODT} of a block copolymer may be determined by the critical temperature at which the value of G' drops precipitously in the plot of G' versus temperature. Using such an empirical rheological criterion that has no theoretical basis, we determine (i) $T_{ODT} \approx 92$ °C for the 25/75 (SB-9/8)/(SI-7/8) blend, (ii) $T_{ODT} \approx 105$ °C for the 50/50 (SB-9/8)/(SI-7/8) blend, and (iii) $T_{ODT} \approx 113$ °C for the 75/25 (SB-9/8)/(SI-7/8) blend.

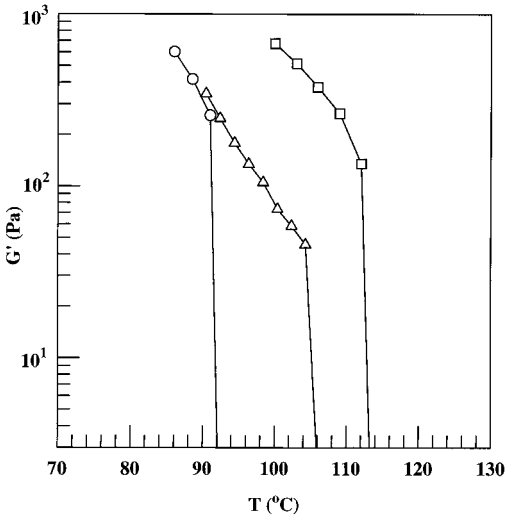

Figure 1. Dependence of G' on temperature for the (SB-9/8)/(SI-7/8) blends obtained from the dynamic temperature sweep experiment under isochronal conditions at $\omega = 0.01$ rad/s: (○) 25/75 (SB-9/8)/(SI-7/8) blend annealed at 85 °C for 7 days, (△) 50/50 (SB-9/8)/(SI-7/8) blend annealed at 90 °C for 5 days, and (□) 75/25 (SB-9/8)/(SI-7/8) blend annealed at 90 °C for 3 days.

Figure 2 gives log G' versus log G'' plots for the 50/50 (SB-9/8)/(SI-7/8) blend at various temperatures ranging from 90 to 120 °C, which were obtained from dynamic frequency sweep experiments at values of ω ranging from 0.01 to 100 rad/s at each temperature chosen. Following Neumann et al.,[33] the log G' versus log G'' plot below will be referred to as the Han plot. It can be seen in Figure 2 that the Han plot has a slope less than 2 at 90−104 °C, makes a sudden downward shift, giving rise to a slope of 2 in the terminal region, as the temperature is increased from 104 to 109 °C, and then remains there with a further increase in temperature, i.e., the Han plot begins to be independent of temperature at 109 °C during heating. Earlier, Han and coworkers[34] suggested that the threshold temperature at which the Han plot during heating becomes independent of temperature be used to determine the T_{ODT} of a block copolymer. It should be pointed out that such a rheological criterion has as its basis a molecular viscoelasticity theory.[35,36] Thus, using Han's rheological criterion, from Figure 2, we determine the T_{ODT} of the 50/50 (SB-9/8)/(SI-7/8) blend to be ca. 109 °C. This value is very close to that (≈105 °C) determined from Figure 1. Using Han plots, not presented here, we determined the T_{ODT}'s for the 25/75 and 75/25 (SB-9/8)/(SI-7/8) blends, as well as for neat block copolymers SB-9/8 and SI-7/8, the results of which are summarized in Table 4. We have

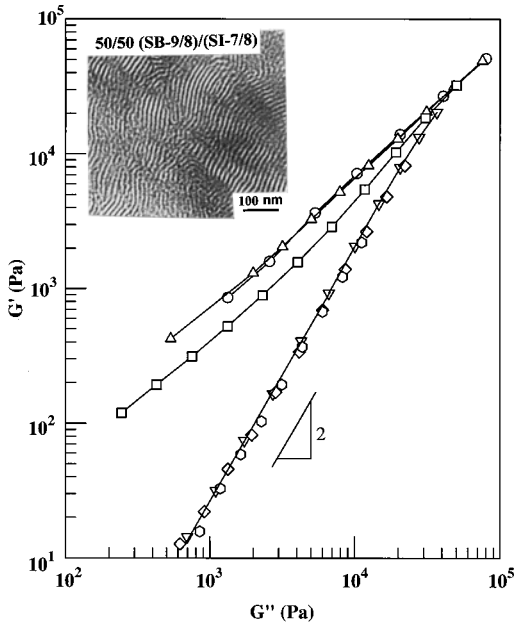

Figure 2. Han plots for the 50/50 (SB-9/8)/(SI-7/8) blend at various temperatures: ○, 90; △, 96; □, 104; ▽, 109; ◇, 114; and ⬡, 120 °C. The specimens used for both the rheological measurements and TEM were annealed at 90 °C for 5 days.

Table 4. Summary of the T_{ODT}'s Determined from Han Plot for the Binary Blends of Diblock Copolymers Investigated

	sample code	w_{C1}[a]	T_{ODT} (°C)[b]
(a)	(SB-9/8)/(SI-7/8) blends		
	SB-9/8		123
	SI-7/8		84
	25/75 (SB-9/8)/(SI-7/8)	0.25	96
	50/50 (SB-9/8)/(SI-7/8)	0.50	109
	75/25(SB-9/8)/(SI-7/8)	0.75	113
(b)	(SI-10/53)/(SB-5/36) blends		
	SI-10/53		185[c]
	SB-5/36		118[c]
	20/80 (SI-10/53)/(SB-5/36)	0.20	151[c]
	40/60 (SI-10/53)/(SB-5/36)	0.40	164[c]
	60/40 (SI-10/53)/(SB-5/36)	0.60	176[c]
	80/20 (SI-10/53)/(SB-5/36)	0.80	180[c]
(c)	(SB-10/10)/(SB-9/8) blends		
	SB-10/10		179
	SB-9/8		123
	25/75 (SB-10/10)/(SB-9/8)	0.25	135
	50/50 (SB-10/10)/(SB-9/8)	0.50	151
	75/25 (SB-10/10)/(SB-9/8)	0.75	162

[a] Weight fraction of block copolymer 1 in the binary mixture. [b] Determined from Han plot. [c] This being a sphere-forming, highly asymmetric diblock copolymer, the temperature given here represents T_{DMT}.

found that values of T_{ODT} determined from Han plots agree well, within experimental uncertainties, with those determined from dynamic temperature sweep experiments. Previously, similar agreement between the two different rheological methods was reported for tri-[34c] and diblock copolymers[37] with lamellar or cylindrical microdomains.

Also given in Figure 2 is a TEM image of the 50/50 (SB-9/8)/(SI-7/8) blend, showing a lamellar microdomain structure, which is indistinguishable from that of the neat diblock copolymers. This observation indicates that the two lamella-forming diblock copolymers, SI-7/8 and SB-9/8, are homogeneously mixed on a segmental level during solvent casting and that there was no macrophase separation.

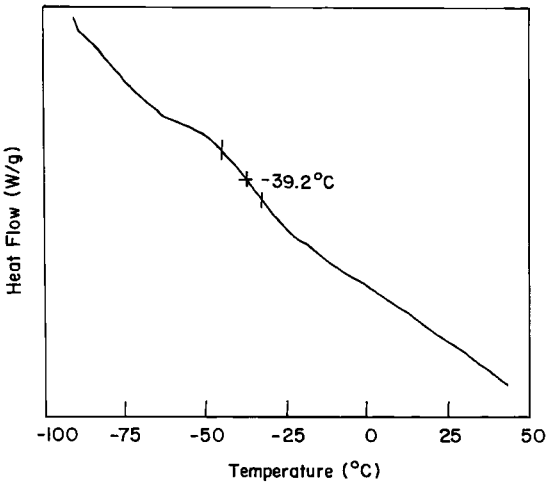

Figure 3. DSC trace for the 50/50 (SB-9/8)/(SI-7/8) blend during heating at a rate of 20 °C/min.

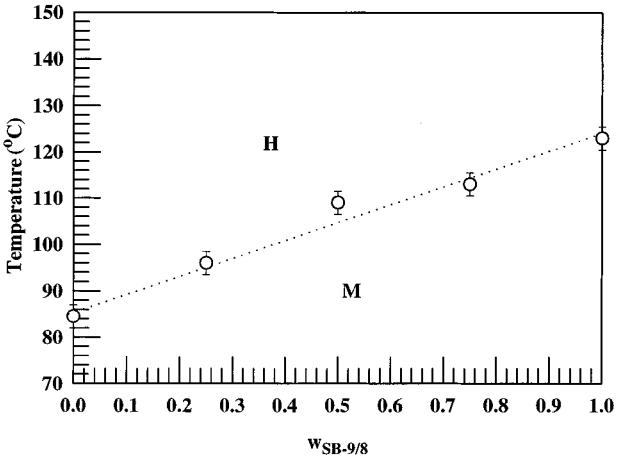

Figure 4. Temperature−composition phase diagram for the (SI-7/8)/(SB-9/8) blends, where H denotes the homogeneous state and M denotes the mesophase. The symbol ○ denotes values of T_{ODT} obtained from the Han plot.

To further ascertain the absence of macrophase separation in (SB-9/8)/(SI-7/8) blends (i.e., to clarify whether the PB block in SB-9/8 and the PI block in SI-7/8 were mixed on a segmental level), we conducted DSC experiments. A DSC trace for the 50/50 (SB-9/8)/(SI-7/8) blend is given in Figure 3, showing a single value of T_g at − 39.2 °C. In view of the fact that the T_g of 1,4-PI is −68 °C and the T_g of 1,2-PB is −12 °C, the T_g of −39.2 °C for the 50/50 (SB-9/8)/(SI-7/8) blend is very reasonable, supporting our conclusion based on the TEM image that (SB-9/8)/(SI-7/8) blends are homogeneously mixed on a segmental level during solvent casting and that there was no macrophase separation.

Figure 4 gives temperature−composition phase diagram for the (SB-9/8)/(SI-7/8) blend system, which was obtained from the values of T_{ODT} determined from rheological measurements. In Figure 4, H denotes the homogeneous phase and M denotes mesophase. It is of great interest to observe in Figure 4 that a nearly linear relationship, within experimental uncertainties, exists between the T_{ODT} and blend composition for the (SB-9/8)/(SI-7/8) system. Below, we will offer a theoretical interpretation of the nearly linear relationship in the temperature−composition phase diagram.

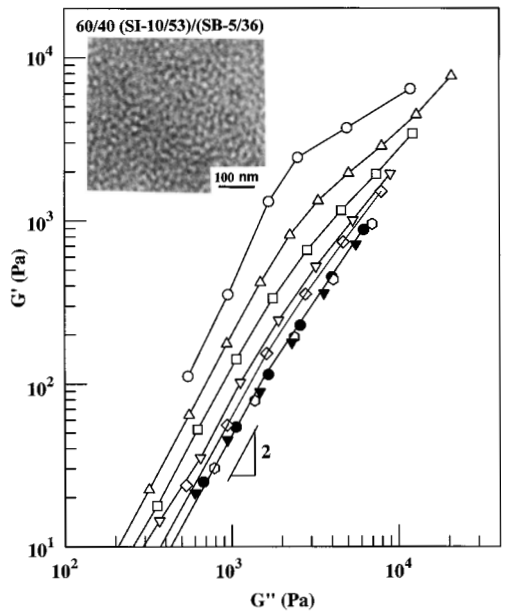

Figure 5. Han plots for the 60/40 (SI-10/53)/(SB-5/36) blend at various temperatures: ○, 111; △, 141; □, 155; ▽, 166; ◇, 171; ⬡, 176; ●, 181; and ▼, 186 °C. The specimens used for both the rheological measurements and TEM were annealed at 70 °C for 2 days.

Phase Diagram for the (SI-10/53)/(SB-5/36) Blend System. The rationale behind the selection of this blend system lies in that both SI-10/53 and SB-5/36 are highly *asymmetric* in composition and have different chemical structures. As summarized in Table 3, the SI-10/53 contains 94% 1,4-addition in PI block and the SB-5/36 contains 86% 1,2-addition in PB block. Thus, for the sake of our discussion below, we will assume that the SI-10/53 is very close to a PS-*block*-1,4-PI copolymer and the SB-5/36 is very close to a PS-*block*-1,2-PB copolymer. Thus, (SI-10/53)/(SB-5/36) blends represent (A-*block*-B)/(A-*block*-C) blends.

Figure 5 gives Han plots for the 60/40 (SI-10/53)/(SB-5/36) blend at various temperatures ranging from 111 to 186 °C, which were obtained from the dynamic frequency sweep experiments at values of ω ranging from 0.01 to 100 rad/s at each temperature. What is of great interest in Figure 5 is that the parallel downward shift of the Han plot having a slope of 2 in the terminal region continues from 141 to 176 °C and then remains there with a further increase in temperature; i.e., the Han plot begins to be independent of temperature at 176 °C during heating. Notice the difference in temperature dependence of the Han plot between lamella-forming block copolymer blends given in Figure 2 and sphere-forming block copolymer blends given in Figure 5; namely, in Figure 2 there is no parallel feature in Han plot, which begins to be independent of temperature at 109 °C. According to our previous studies that employed small-angle X-ray scattering (SAXS) and TEM on a highly asymmetric SIS triblock copolymer[38] and highly asymmetric SI diblock copolymers,[39] the block copolymers still maintained a sharp interface at temperatures between the onset and completion of the parallel shift of Han plot, although the long-range body-centered cubic phase was lost. That is, at the onset of the parallel feature of Han plot, spherical microdomains in a highly asymmetric block copolymer begin to transform, as determined from SAXS and TEM, into distorted microdomains with short-range liquidlike spatial order.

What is significant in Figure 5 is that there exists a critical temperature (176 °C), at and above which the Han plot begins to be independent of temperature, very similar to that observed in Figure 2. Thus, if we apply to Figure 5 the same rheological criterion as that applied to Figure 2, we conclude that the 60/40 (SI-10/53)/(SB-5/36) blend forms a homogeneous phase at 176 °C but not at 141 °C, because the Han plot begins to be independent of temperature at 176 °C; i.e., at 176 °C, the microdomain structures of the 60/40 (SI-10/53)/(SB-5/36) blend with short-range order disappear and are transformed into the homogeneous state in which the component polymers are mixed on a molecular level and only thermally induced composition fluctuations may exist. Following our previous study,[39] in reference to Figure 5, we determine 141 °C to be the lattice disordering/ordering transition (LDOT) temperature (T_{LDOT}) and 176 °C to be the demicellization/micellization transition (DMT) temperature (T_{DMT}). It should be mentioned that the T_{DMT} of highly *asymmetric* block copolymer is equivalent to the T_{ODT} of *symmetric* or *nearly symmetric* block copolymer, which does not undergo lattice disordering/ordering transition. Using Han plots, not presented here, we determined the T_{DMT}'s for the 20/80, 40/60, and 80/20 (SI-10/53)/(SB-5/36) blends, the results of which are summarized in Table 4.

We wish to mention that DMT may not be a true phase transition from a rigorous thermodynamic point of view, whereas LDOT is a true thermodynamic phase transition. DMT may be regarded as a pseudo-phase transition, involving effectively a *finite* number of molecules and hence occurring over a *finite* range (possibly a narrow range) of temperatures.[39] Nevertheless, we wish to make a distinction between LDOT and DMT in *highly asymmetric* block copolymers, because we believe that the mechanism associated with phase transitions in highly asymmetric block copolymers is quite different from that in symmetric or nearly symmetric block copolymers. We are well aware of the fact that at present there exists no space group that can be assigned to distorted spheres or disordered arrangement of spheres with short-range liquidlike order (termed disordered spheres or micelles). We do not believe that anyone has a definitive answer as to whether micelles form continuously as the temperature is lowered or if micelles dissolve continuously into a micelle-free homogeneous phase as the temperature is increased. Further, there is no reason a thermodynamically sharp temperature cannot exist at which micelles suddenly form from or dissolve into the micelle-free homogeneous phase. At present, we simply do not have adequate experimental techniques available to determine a sharp discontinuity in temperature at which micelles may suddenly form or disappear. We do not believe that anyone can deny that the formation of micelles from a homogeneous phase and the disappearance of micelles are phase-transitions.

Also given in Figure 5 is a TEM image of the 60/40 (SI-10/53)/(SB-5/36) blend, showing distorted microdomains with short-range spatial order. This observation indicates that the two block copolymers, SI-10/53 and SB-5/36, are homogeneously mixed at a segmental level during solvent casting and that there was no macrophase separation. To clarify whether the PI block in SI-10/53 and the PB block in SB-5/36 were mixed on a segmental level, we conducted DSC experiments. A DSC trace for the 40/60 (SI-10/53)/(SB-5/36) blend is

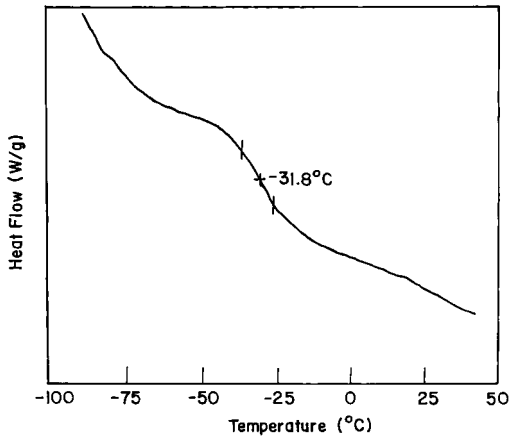

Figure 6. DSC trace for the 40/60 (SI-10/53)/(SB-5/36) blend during heating at a rate of 20 °C/min.

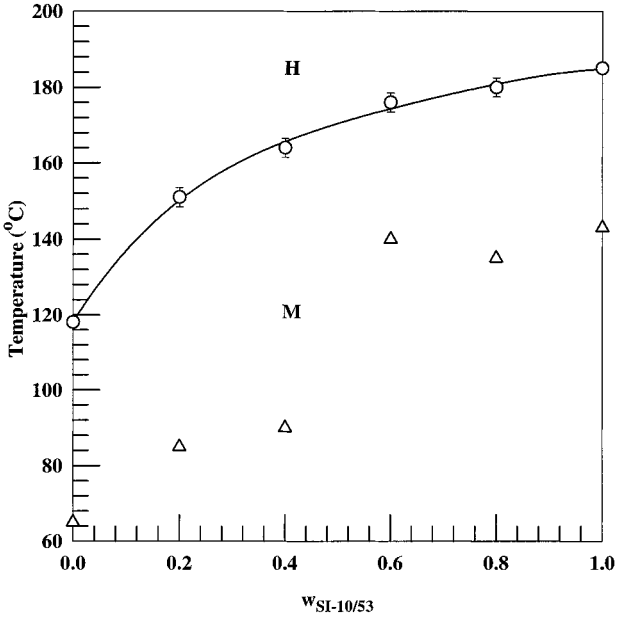

Figure 7. Temperature−composition phase diagram for the (SI-10/53)/(SB-5/36) blends, where H denotes the homogeneous state and M denotes the mesophase. The open circle ○ denotes values of the temperature (i.e., T_{MDT}) at which the Han plot having a slope of 2 in the terminal region begins to be independent of temperature during heating, and the open triangle △ denotes the temperature at which the Han plot first exhibits a slope of 2 in the terminal region during heating.

given in Figure 6, showing a single value of T_g at −31.8 °C. In view of the fact that the T_g of 1,4-PI is −68 °C and the T_g of 1,2-PB is −12 °C, the T_g of −31.8 °C for the 40/60 (SI-10/53)/(SB-5/36) blend is very reasonable, supporting our conclusion based on the TEM image that (SI-10/53)/(SB-5/36) blends are homogeneously mixed on a segmental level during solvent casting and that there was no macrophase separation.

Figure 7 gives temperature−composition phase diagram for the (SI-10/53)/(SB-5/36) blend system, in which the symbol ○ denotes the values of T_{DMT} (see Table 1) determined from Han plots using the rheological criterion described above. It is of great interest to note in Figure 7 that the temperature−composition phase diagram for the (SI-10/53)/(SB-5/36) blend system, drawn by a solid line, shows *positive* deviation from linearity, quite different from the nearly linear relationship observed in Figure 4 for the (SB-9/8)/(SI-7/8) blend

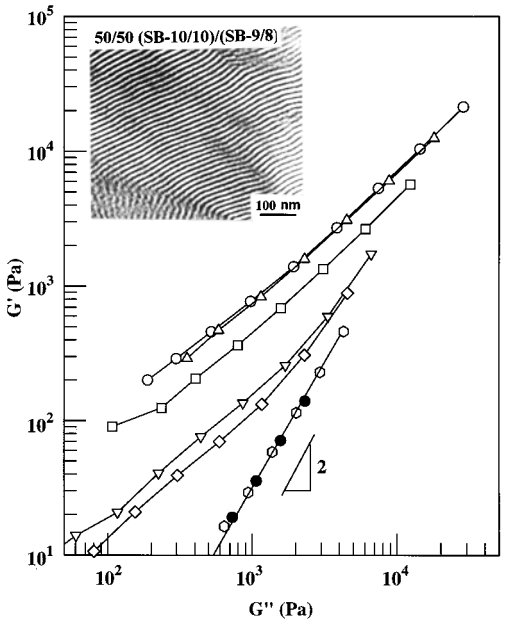

Figure 8. Han plots for the 50/50 (SB-10/10)/(SB-9/8) blend at various temperatures: ○, 121; △, 131; □, 136; ▽, 141; ◇, 146; ⬡, 151; and ●, 158 °C. The specimens used for both the rheological measurements and TEM were annealed at 100 °C for 3 days.

system. The major difference between the two blend systems lies in that both block copolymers, SI-10/53 and SB-5/36, are highly asymmetric, whereas both block copolymers, SB-9/8 and SI-7/8, are nearly symmetric. The observed difference in temperature−composition phase diagrams between the two blend systems can be explained by random phase approximation (RPA) calculations, as will be discussed below. Also given in Figure 7, for comparison, are the data points (the symbol △) which were determined from the temperature (i.e., T_{LDOT}) at which the Han plot begins to exhibit a parallel feature in the heating process. It can be seen that such data points show no correlation in the temperature−composition phase diagram, supporting our contention that T_{LDOT} is not equivalent to T_{ODT} for *highly asymmetric* block copolymers.

Phase Diagram for (SB-10/10)/(SB-9/8) Blend System. The rationale behind the selection of this blend system lies in that both block copolymers are *nearly symmetric* in composition but have different microstructures in the PB block of the respective copolymers. As summarized in Table 3, SB-10/10 has very low vinyl content (9% 1,2-addition) and SB-9/8 has very high vinyl content (89% 1,2-addition). Thus, for the sake of our discussion below, we will assume that the SB-10/10 is very close to a PS-*block*-1,4-PB copolymer and the SB-9/8 is very close to a PS-*block*-1,2-PB copolymer. Thus, (SB-10/10)/(SB-9/8) blends represent (A-*block*-B)/(A-*block*-C) blends.

Figure 8 gives Han plots for the 50/50 (SB-10/10)/(SB-9/8) blend at various temperatures ranging from 121 to 158 °C, which were obtained from the dynamic frequency sweep experiments at values of ω ranging from 0.01 to 100 rad/s at each temperature. It can be seen from Figure 8 that the Han plot having a slope of 2 in the terminal region begins to be independent of temperature at 151 °C and remains there with further increases in temperature. Following Han's rheological criterion,[34] we determine the T_{ODT} of the 50/50 (SB-10/

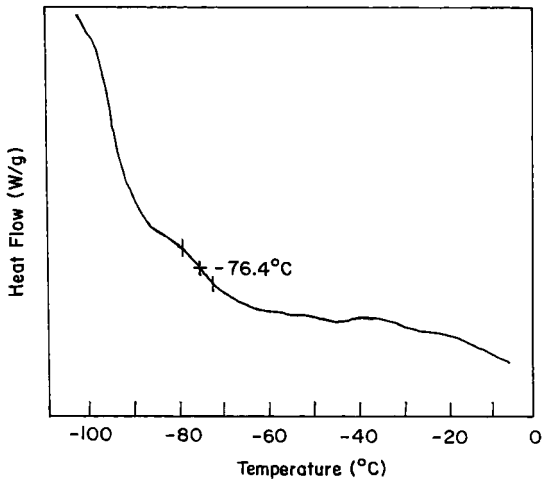

Figure 9. DSC trace for the 50/50 (SB-10/10)/(SB-9/8) blend during heating at a rate of 20 °C/min.

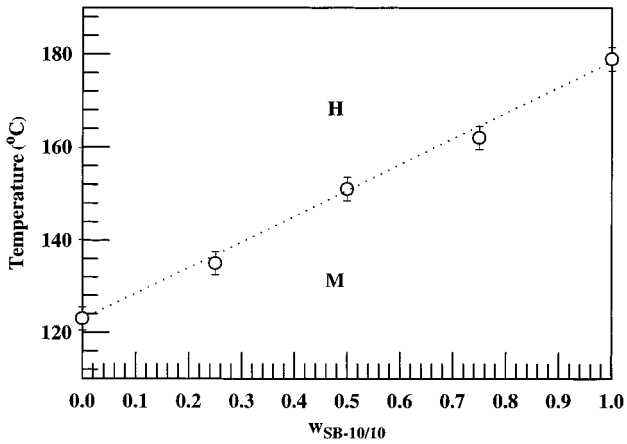

Figure 10. Temperature−composition phase diagram for the (SB-10/10)/(SB-9/8) blends, where H denotes the homogeneous state and M denotes the mesophase. The symbol ○ denotes values of the T_{ODT} obtained from the Han plot.

10)/(SB-9/8) blend to be ca. 151 °C. Using Han plots, not presented here, we determined the T_{ODT}'s for the 25/75 and 75/25 (SB-10/10)/(SB-9/8) blends, the results of which are summarized in Table 4.

Also given in Figure 8 is a TEM image of the 50/50 (SB-10/10)/(SB-9/8) blend, showing lamellar microdomains. Recall that neat block copolymers SB-10/10 and SB-9/8 have lamellar microdomain structure. This observation indicates that the two block copolymers, SB-10/10 and SB-9/8, are homogeneously mixed at a segmental level during solvent casting and that there was no macrophase separation. To clarify whether the 1,4-PB block in SB-10/10 and the 1,2-PB block in SB-9/8 were mixed on a segmental level, we conducted DSC experiments. A DSC trace for the 50/50 (SB-10/10)/(SB-9/8) blend is given in Figure 9, showing a single value of T_g at −76.4 °C. It should be remembered that SB-10/10 consists of ca. 91% 1,4-PB and ca. 9% 1,2-PB, and SB-9/8 consists of ca. 89% 1,2-PB and ca. 11% 1,4-PB (see Table 1). In view of the fact that the T_g of 1,4-PB is −98 °C and the T_g of 1,2-PB is −12 °C, the T_g of −76.4 °C for the 50/50 (SB-10/10)/(SB-9/8) blend is reasonable, supporting our conclusion based on the TEM image that (SB-10/10)/(SB-9/8) blends are homogeneously mixed on a segmental level during solvent casting and that there was no macrophase separation.

Figure 10 gives a temperature−composition phase diagram for the (SB-10/10)/(SB-9/8) blends. It is of great interest to observe in Figure 10 that the temperature−composition phase diagram for the (SB-10/10)/(SB-9/8) blend system shows a nearly linear relationship, very similar to that for the (SB-9/8)/(SI/7/8) blend system given in Figure 4. Note that both block copolymers, SB-10/10 and SB-9/8, are nearly symmetric in composition (see Table 1) as are the block copolymers SB-9/8 and SI/7/8. Below, we will interpret the composition-dependent phase diagram using RPA calculations.

Miscibility Limits and Macrophase Separation in Binary Blends of Block Copolymers. The miscibility of (PS-*block*-PI)$_1$/(PS-*block*-PI)$_2$ blends was investigated extensively by Hashimoto et al.[5] According to their study, when $f_{PS,1}$ and $f_{PS,2}$ in the two SI diblock copolymers were in the range of 0.35−0.69, the miscibility was found to be dependent upon the molecular weight ratio of the two diblock copolymers, the $M_{C,1}/M_{C,2}$ ratio. When the $M_{C,1}/M_{C,2}$ ratio was less than 5, the two diblock copolymers were found to be totally miscible, giving rise to a single phase with a uniform microdomain structure even when $f_{PS,1}$ and $f_{PS,2}$ were vastly different ($f_{PS,1} = 0.69$ and $f_{PS,2} = 0.35$). In that case, the morphology was found to vary, depending upon the total volume fraction of PS block in the binary blend (ϕ_{PS}^T). When the $M_{C,1}/M_{C,2}$ ratio exceeded 10, the (PS-*block*-PI)$_1$/(PS-*block*-PI)$_2$ blends were found to be only partially miscible, even when $f_{PS,1}$ and $f_{PS,2}$ were almost identical ($f_{PS,1} = 0.49$ and $f_{PS,2} = 0.48$) and underwent macrophase separation.

The above experimental observations by Hashimoto et al.[5] seem to explain why we did not observe macrophase separation in our blend systems, because the $M_{C,1}/M_{C,2}$ ratio is less than 1.6 and the difference between $f_{PS,1}$ and $f_{PS,2}$, $|f_{PS,1} - f_{PS,2}|$, is very small (≤ 0.05) in our blend systems (see Table 2). We are well aware of the fact that, strictly speaking, the experimental results of Hashimoto et al.[5] on the (PS-*block*-PI)$_1$/(PS-*block*-PI)$_2$ blend system may not be applicable to our (A-*block*-B)/(A-*block*-C) blend system. Below, however, using the results of RPA calculations we will show that differences between the (PS-*block*-PI)$_1$/(PS-*block*-PI)$_2$ blend system investigated by Hashimoto et al.[5] and our (A-*block*-B)/(A-*block*-C) blend system are very small. This is because, besides the low $M_{C,1}/M_{C,2}$ ratio and small values of $|f_{PS,1} - f_{PS,2}|$ in our blend systems, there are thermodynamic reasons. Specifically, for the (SB-9/8)/(SI-7/8) blend system, the 1,2-PB segment of SB-9/8 and the 1,4-PI segment of SI-7/8 have attractive interactions (i.e., negative value of the Flory−Huggins interaction parameter χ),[30] whereas the PS and 1,2-PB segments of SB-9/8, and the PS and 1,4-PI segments of SI-7/8 have strong repulsive interactions (i.e., positive value of χ).[34c,40] The same argument holds for the (SI-10/53)/(SB-5/36) blend system. For the (SB-10/10)/(SB-9/8) blend system, the 1,4-PB segment of SB-10/10 and the 1,2-PB segment of SB-9/8 have extremely weak repulsive interactions,[31] whereas the PS and 1,4-PB segments of SB-10/10 and the PS and 1,2-PB segments of SB-9/8 have strong repulsive interactions.[40] Specifically, we observe that at 100 °C $\chi = 0.829 \times 10^{-2}$ for the (1,2-PB)/(1,4-PB) pair, while $\chi = 0.1448$ for the PS/(1,2-PB) pair and $\chi = 0.1037$ for the PS/(1,4-PB) pair. These values of χ are obtained from the expressions for the interaction parameters given in Table 5.

RPA Calculations for Binary Blends of Block Copolymers. At present, there exists no comprehensive

Table 5. Expressions Used for the Interaction Parameter

polymer pair	interaction parameter	eq	ref
PS/(1,4-PI)[a]	$\alpha = -0.118 \times 10^{-2} + 0.839/T$	1	34c
PS/(1,2-PB)[b]	$\alpha = -0.1699 \times 10^{-2} + 1.0895/T + 0.0351\phi_{PS}/T$	2	40
PS/(1,4-PB)[c]	$\alpha = -0.1632 \times 10^{-2} + 0.9441/T + 0.0755\phi_{PS}/T$	3	40
(1,2-PB)/(1,4-PB)	$\chi = 0.679 \times 10^{-2} + 0.561/T$	4	31
(1,4-PI)[a]/(1,2-PB)[d]	$\chi = 0.7905 \times 10^{-2} - 3.82/T - 0.1394\phi_{PB}/T$	5	this study

[a] PI having 96% 1,4-addition and 6% 3,4-addition. [b] PB having 93% 1,2-addition. [c] PB having 7% 1,2-addition and 93% 1,4-addition. [d] PB having 90% 1,2-addition. α is related to χ from the following relationship, $\chi = \alpha V_{ref}$ with V_{ref} being the molar volume of a reference component. ϕ_{PS} is volume fraction of PS. ϕ_{PB} is volume fraction of PB. T is the absolute temperature.

theory predicting temperature−composition phase diagrams for the (A-*block*-B)/(A-*block*-C) blend system. In the present study, we used the scattering functions reported by Kim et al.[41] to carry out RPA calculations for the (A-*block*-B)/(A-*block*-C) blend system. Although we realize RPA calculations only provide stability limits and not the equilibrium phase diagrams, we have found the RPA calculations to be very helpful in interpreting the experimental temperature−composition phase diagrams given in Figures 4, 7, and 10. It should be emphasized that the primary objective of the RPA calculations is to assess whether the phase diagrams presented above are reasonable, so that they will be useful to future theoretical development.

The results of RPA calculations are summarized in Figure 11. In carrying out RPA calculations, we needed expressions for (i) the temperature-dependent interaction parameters for the PS/(1,4-PI), PS/(1,2-PB), PS/(1,4-PB), (1,2-PB)/(1,4-PB), and (1,4-PI)/(1,2-PB) pairs and (ii)the temperature-dependent specific volumes of PS, 1,4-PI, 1,2-PB, and 1,4-PB. Table 5 gives the expressions for the interaction parameters used, and Table 6 gives the expressions for the specific volumes used. It should be mentioned that the prediction of phase behavior in blends of two homopolymers or blends of two block copolymers would depend on the specific expressions for the interaction parameter employed.

Two experimental methods have been used to determine values of the interaction parameter, χ or α: (i) cloud point measurement for a pair of homopolymers (say A and B) and (ii) radiation scattering measurement for an AB-type diblock copolymer, namely, SAXS or small-angle neutron scattering (SANS). The cloud point measurement makes use of the Flory−Huggins equilibrium thermodynamic theory, and the radiation scattering method makes use of the RPA theory of Leibler.[43] χ (or α) may depend not only on temperature but also on blend (or block copolymer) composition[30,40] and the molecular weight of the constituent components.[44] It is reported in the literature[37] that the expressions for χ determined from SAXS experiment differ greatly depending on the sources. Sometimes the same investigators, using SAXS, reported different expressions for χ for slightly different molecular weights of SI block copolymers. A serious question may be raised as to which of the two methods, cloud point or radiation scattering, would be more suitable to determine the interaction parameter, to predict phase behavior of block copolymers. A recent study of Maurer et al.[45] reports that they obtained four different temperature-dependent expressions for χ from SANS based on the Leibler

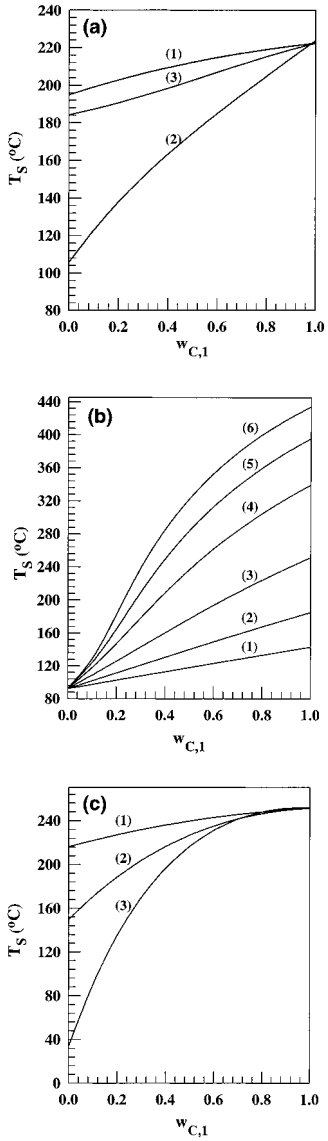

Figure 11. (a) Plots of T_s versus w_{C1} (spinodal curves) predicted from RPA calculations: curve 1 for the (SB-9/8)/(SI-9/8) blend system, curve 2 for the (SI-10/53)/(SB-5/36) blend system, and curve 3 for (SB-10/10)/(SB-9/8) blend. The molecular weights of the block copolymer used for the RPA calculations are given in Table 1, and values of $Z_{C,1}/Z_{C,2}$ ratio and $(w_{PS,1} - w_{PS,2})$ for each polymer pair are given in Table 2. (b) Effect of Z_{C1}/Z_{C2} ratio on T_s versus $w_{C,1}$ plots (spinodal curves) predicted from RPA calculations for the (PS-*block*-PI)$_1$/(PS-*block*-PI)$_2$ blend system with fixed molecular weights of (PS-*block*-PI)$_2$ = 8000PS-*block*-8000PI and fixed block compositions $w_{PS,1} = w_{PS,2} = 0.5$: curve 1 for $Z_{C,1}/Z_{C,2} = 1.25$, curve 2 for $Z_{C,1}/Z_{C,2} = 1.5$, curve 3 for $Z_{C,1}/Z_{C,2} = 2$, curve 4 for $Z_{C,1}/Z_{C,2} = 3$, curve 5 for $Z_{C,1}/Z_{C,2} = 4$, and curve 6 for $Z_{C,1}/Z_{C,2} = 5$. (c) Effect of $|f_{PS,1} - f_{PS,2}|$ on T_s versus $w_{C,1}$ plots (spinodal curves) predicted from RPA calculations for the (PS-*block*-PI)$_1$/(PS-*block*-PI)$_2$ blend system with fixed molecular weights of (PS-*block*-PI)$_1$ = 16 000PS-*block*-16 000PI ($w_{PS,1} = 0.5$) and $Z_{C,1} = Z_{C,2} = 388$, but varying block compositions of (PS-*block*-PI)$_2$: curve 1 for $w_{PS,1} - w_{PS,2} = 0.094$, curve 2 for $w_{PS,1} - w_{PS,2} = 0.184$, and curve 3 for $w_{PS,1} - w_{PS,2} = 0.282$.

theory,[43] but a single expression for χ from cloud point measurement. They concluded that the deficiencies of the Leibler theory and fluctuation-corrected version might be responsible for not being able to obtain a single expression for χ from SANS experiments. They suggested that a more comprehensive block copolymer theory that takes into account chain polarization and

Table 6. Expressions Used for the Specific Volume

polymer	specific volume (cm^3/g)	eq	ref
PS	$v_{PS} = 0.9217 + 5.412 \times 10^{-4}(T - 273) + 1.687 \times 10^{-7}(T - 273)^2$	6	42
1,4-PI	$v_{1,4-PI} = 1.0771 + 7.22 \times 10^{-4}(T - 273) + 2.46 \times 10^{-7}(T - 273)^2$	7	34c
1,2-PB	$v_{1,2-PB} = 1.1072 + 8.19 \times 10^{-4}(T - 273)$	8	42
1,4-PB	$v_{1,4-PB} = 1.1138 + 8.24 \times 10^{-4}(T - 273)$	9	this study

stretching in the vicinity of ODT be developed in the future. We infer from the conclusions of Maurer et al.[45] that in order to compare theory with experiment the expressions for α determined from cloud point measurements for binary blends would give more accurate prediction of phase behavior of block copolymers than the expressions for χ determined from SAXS or SANS measurements for diblock copolymers.

Figure 11a gives the results of RPA calculations in terms of the spinodal temperature (T_s) for microphase separation and the weight fraction of block copolymer 1, $w_{C,1}$. In Figure 11a, curve 1 represents the (SB-9/8)/(SI-7/8) blend system, curve 2 represents the (SI-10/53)/(SB-5/36) blend system, and curve 3 represents the (SB-10/10)/(SB-9/8) blend system. It should be mentioned that the RPA calculations indicated *no* macrophase separation to occur in any of the three blend systems investigated, which is consistent with our TEM results. It is of interest to observe in Figure 11a that T_s versus $w_{C,1}$ plots show a very weak positive deviation from linearity for all three blend systems, although the (SI-10/53)/(SB-5/36) blend system (curve 2) gives a slightly greater deviation from linearity than the other two blend systems. These results are in qualitative agreement with the experimental results given in Figures 4, 7, and 10.

Figure 11b describes the effect of the $Z_{C,1}/Z_{C,2}$ ratio on T_s versus $w_{C,1}$ plots, obtained from RPA calculations, for the (PS-*block*-PI)$_1$/(PS-*block*-PI)$_2$ blend system having $f_{PS,1} = f_{PS,2} = 0.5$. It can be seen in Figure 11b that the T_s versus w_{C1} plot virtually follows a linear relationship for $Z_{C,1}/Z_{C,2} \leq 1.25$ and begins to exhibit *positive* deviation from linearity as the $Z_{C,1}/Z_{C,2}$ ratio is increased from 1.25 to 2 and higher. Note that Figure 11b was obtained for $|f_{PS,1} - f_{PS,2}| = 0$.

Figure 11c describes the effect of $|f_{PS,1} - f_{PS,2}|$ on T_s versus $w_{C,1}$ plots, obtained from RPA calculations, for the (PS-*block*-PI)$_1$/(PS-*block*-PI)$_2$ blend system having a fixed value of $Z_{C,1} = Z_{C,2} = 388$. It can be seen in Figure 11c that $|f_{PS,1} - f_{PS,2}|$ has a profound influence on the shape of the phase diagram, showing that the extent of positive deviation from linearity in T_s versus $w_{C,1}$ plots increases with increasing $|f_{PS,1} - f_{PS,2}|$ from 0.094 to 0.282. Comparison of Figure 11c with Figure 11b indicates that $|f_{PS,1} - f_{PS,2}|$ has a much greater influence on the shape of the phase diagram for the (A-*block*-B)$_1$/(A-*block*-B)$_2$ blend system than that of the $Z_{C,1}/Z_{C,2}$ ratio.

It is appropriate to discuss at this juncture the experimentally determined temperature−composition phase diagrams for (A-*block*-B)$_1$/(A-*block*-B)$_2$ blend systems reported by previous investigators. Using SAXS, Floudas et al.[17] observed a linear relationship in the temperature−composition phase diagram for the (PS-*block*-PI)$_1$/(PS-*block*-PI)$_2$ blend system having $Z_{C,1}/Z_{C,2} = 0.74$, $f_{PS,1} = 0.53$, and $f_{PS,2} = 0.54$. Their experimental results are consistent with the RPA calculations given in Figure 11b. On the other hand, Almdal et al.[16] reported negative deviation from linearity in the temperature−composition phase diagram for binary blends consisting of nearly *symmetric* poly(ethylene propylene)-*block*-poly(ethyl ethylene) (PEP-*block*-PEE) copolymers, i.e., a (A-*block*-B)$_1$/(A-*block*-B)$_2$ blend system. As can be seen in Figure 11b,c, the RPA calculations do *not* predict negative deviation from linearity in the temperature−composition phase diagram for the (A-*block*-B)$_1$/(A-*block*-B)$_2$ blend system, leading us to conclude that the values of T_{ODT} determined by Almdal et al.[16] might not have been accurate.

It is appropriate to mention at this juncture that earlier, using SAXS and Han plots, Yamaguchi et al.[18] observed very strong positive deviation from linearity, going through a maximum, in the temperature−composition phase diagram for a (PS-*block*-PI)$_1$/(PS-*block*-PI)$_2$ blend system having $Z_{C,1}/Z_{C,2} = 2.16$ and $|f_{PS,1} - f_{PS,2}| = 0.322$. Such an experimental observation is predicted by RPA calculations,[18] although not presented here.

Concluding Remarks

In this paper, we have presented temperature−composition phase diagrams for binary blends of chemically dissimilar diblock copolymers, (A-*block*-B)/(A-*block*-C) blends. We determined the phase boundary between the mesophase and homogeneous phase using oscillatory shear rheometry, which enabled us to construct temperature−composition phase diagrams in the absence of macrophase separation. Our experimental results indicate that the difference in block length ratio of two block copolymers has a greater influence on the shape of temperature−composition phase diagrams than the difference in degree of polymerization. We found further that blends of highly *asymmetric* diblock copolymers have a greater influence on the shape of temperature−composition phase diagrams than blends of nearly *symmetric* block copolymers. Specifically, blends of nearly *symmetric* diblock copolymers (i.e., $f_{PS} \approx 0.5$) with $Z_{C,1}/Z_{C,2} \leq 1.5$ show an almost linear relationship between temperature and composition.

We found that isochronal dynamic temperature sweep experiment cannot be used to determine the T_{DMT} (corresponding to the T_{ODT} of symmetric or nearly symmetric block copolymer) of a *highly asymmetric* diblock copolymer. Thus, we had to perform dynamic frequency sweep experiments at various temperatures to determine the T_{DMT}'s of two *highly asymmetric* diblock copolymers, SI-10/53 and SB-5/36, and their binary blends, to determine the phase boundary between the mesophase and homogeneous phase.

We found that both isochronal dynamic temperature sweep experiments and dynamic frequency sweep experiments at various temperatures give rise to virtually identical information on the T_{ODT} of nearly *symmetric* diblock copolymers and their binary blends. This finding will be very useful to those who in the future wish to construct, via rheological method, temperature−composition phase diagrams for binary blends of diblock copolymers.

Acknowledgment. We acknowledge with gratitude that Dr. Steven F. Hahn of Dow Chemical Company supplied us with the SB-10/10 and Dr. Adel Halasa of Goodyear Tire and Rubber Company supplied us with the SB-9/8 and SB-5/36 employed in this study. We acknowledge that the DSC measurements summarized

in Figures 3, 6, and 9 were conducted upon the suggestion of an anonymous reviewer, to whom we are very grateful.

References and Notes

(1) Hashimoto, T.; Tanaka, H.; Hasegawa, H. In *Molecular Conformation and Dynamics of Macromolecules in Condensed Systems*; Nagasawa, M., Ed.; Elsevier: Amsterdam, 1988; p 257.
(2) Ishizu, K.; Omote, A.; Fukutomi, T. *Polymer* **1990**, *31*, 2135.
(3) Kimishima, K.; Jinnai, H.; Hashimoto, T. *Macromolecules* **1970**, *32*, 2585.
(4) Jeon, H. G.; Hudson, S. D.; Ishida, H.; Smith, S. D. *Macromolecules* **1999**, *32*, 1803.
(5) Hashimoto, T.; Yamasaki, K.; Koizumi, S.; Hasegawa, H. *Macromolecules* **1993**, *26*, 2895.
(6) Hashimoto, T.; Koizumi, S.; Hasegawa, H. *Macromolecules* **1994**, *27*, 1562.
(7) Koizumi, S.; Hasegawa, H.; Hashimoto, T. *Macromolecules* **1994**, *27*, 4371.
(8) Vilesov, A. D.; Floudas, G.; Pakula, T.; Melenevskaya, E. Y.; Birshtein, T. M.; Lyatskaya, Y. V. *Macromol. Chem. Phys.* **1994**, *195*, 2317.
(9) Spontak, R. J.; Fung, J. C.; Braunfeld, M. B.; Sedat, J. W.; Agard, D. A.; Kane, L.; Smith, S. D.; Saktowski, M. M.; Ashraf, A.; Hajduk, D. A.; Grunner, S. M. *Macromolecules* **1996**, *29*, 4494.
(10) Kane, L.; Satowski, M. M.; Smith, S. D.; Spontak, R. J. *Macromolecules* **1996**, *29*, 8862.
(11) Koneripalli, N.; Levicky, R.; Bates, F. S.; Matsen, M. W.; Satija. S. K.; Ankner, J.; Kaiser, H. *Macromolecules* **1998**, *31*, 3498.
(12) Sakurai, S.; Irie, H.; Umeda, H.; Nomura, S.; Lee, H. H.; Kim, J. K. *Macromolecules* 1**998**, *31*, 336.
(13) Lin, E. K.; Gast, A. P.; Shi, A- C.; Noolandi, J.; Smith, S. D. *Macromolecules* **1996**, *29*, 5920.
(14) Mayes, A. M.; Russell, T. P.; Deline, V. R.; Satija, S. K.; Majkrzak, C. F. *Macromolecules* **1994**, *27*, 7447.
(15) Tcherkasskaya, O.; Ni, S.; Winnik, M. A. *Macromolecules* **1997**, *30*, 2623.
(16) Almdal, K.; Rosedale, J. H.; Bates, F. S. *Macromolecules* **1990**, *23*, 4336.
(17) Floudas, G.; Vlassopoulos, D.; Pitsikalis, M.; Hadjichristidis, N.; Stamm, M. *J. Chem. Phys.* **1996**, *104*, 2083.
(18) Yamaguchi, D.; Hashimoto, T.; Han, C. D.; Baek, D. M.; Kim, J. K.; Shi, A.-C. *Macromolecules* **1997**, *30*, 5832.
(19) Bodycomb, J.; Yamaguchi, D.; Hashimoto, T. *Polym. J.* **1996**, *28*, 821.
(20) Sakurai, S.; Umeda, H.; Furukawa, C.; Irie, H.; Nomura, S.; Lee, H. H.; Kim, J. K. *J. Chem. Phys.* **1998**, *108*, 4333.
(21) Löwenhaupt, B.; Hellmann, G. P. *Polymer* **1991**, *32*, 1065.
(22) Lyatskaya, Yu. V.; Zhulina, E. B.; Birshtein, T. M. *Polymer* **1992**, *33*, 343.
(23) Birshtein, T. M.; Lyatskaya, Yu. V.; Zhulina, E. B. *Polymer* **1992**, *33*, 2750.
(24) Shi, A.-C.; Noolandi, J. *Macromolecules* **1994**, *27*, 2936.
(25) Shi, A.-C.; Noolandi, J. *Macromolecules* **1995**, *28*, 3103.
(26) Dan, N.; Safran, S. A. *Macromolecules* **1994**, *27*, 5766.
(27) Spontak, R. J. *Macromolecules* **1994**, *27*, 6363.
(28) Matsen, M. W. *J. Chem. Phys.* **1995**, *103*, 3268.
(29) Sakurai, S.; Nomura, S. *Polymer* **1997**, *38*, 4103.
(30) Thudium, R. N.; Han, C. C. *Macromolecules* **1996**, *29*, 2143.
(31) Bates, F. S.; Hartney, M. A. *Macromolecules* **1985**, *18*, 2478.
(32) (a) Gouinlock, E. V.; Porter, R. S. *Polym. Eng. Sci.* **1977**, *17*, 535. (b) Chung, C. I.; Lin, M. I. *J. Polym. Sci., Polym. Phys. Ed.* **1978**, *16*, 545. (c) Widmaier, J. M.; Meyer, G. C. *J. Polym. Sci., Polym. Phys. Ed.* **1980**, *18*, 2217.
(33) Neumann, C.; Loveday, D. R.; Abetz, V.; Stadler, R. *Macromolecules* **1998**, *31*, 2493. These authors referred to the log G' versus log G'' plot as the Han plot. It should be mentioned that the Han plot has no relation whatsoever with the Cole−Cole plot, which gives a temperature-dependent semicircle in rectangular coordinates.
(34) (a) Han, C. D.; Kim, J. *J. Polym. Sci. Part B: Polym. Phys.* **1987**, *25*, 1741. (b) Han, C. D.; Kim, J.; Kim, J. K. *Macromolecules* **1989**, *22*, 383. (c) Han, C. D.; Baek, D. M.; Kim, J. K. *Macromolecules* **1990**, *23*, 561.
(35) Han, C. D.; Jhon, M. S. *J. Appl. Polym. Sci.* **1986**, *32*, 3809.
(36) Han, C. D.; Kim, J. K. *Macromolecules* **1989**, *22*, 4292.
(37) Han, C. D.; Baek, D. M.; Kim, J. K.; Ogawa, T.; Sakamoto, N.; Hashimoto, T. M*acromolecules* **1995**, *28*, 5043.
(38) Sakamoto, N.; Hashimoto, T.; Han, C. D.; Kim, D.; Vaidya, N. Y. *Macromolecules* **1997**, *30*, 1621.
(39) Han, C. D.; Vaidya, N. Y.; Kim, D.; Shin, G.; Yamaguchi, D.; Hashimoto, T. *Macromolecules*, in press.
(40) Han, C. D.; Chun, S. B.; Hahn, S. F.; Harper, S. Q.; Savickas, P. J.; Meunier, D. M.; Li, L.; Yalcin, T. *Macromolecules* **1998**, *31*, 394.
(41) Kim, J. K.; Kimishima, K.; Hashimoto, T. M*acromolecules* **1993**, *26*, 125.
(42) Rigby, D.; Roe, R.-J. *Macromolecules* **1986**, *19*, 721.
(43) Leibler, L. *Macromolecules* **1980**, *13*, 1602.
(44) Mori, K.; Okawara, A.; Hashimoto, T. *J. Chem. Phys.* **1996**, *104*, 7765.
(45) Maurer, W. W.; Bates, F. S.; Lodge, T. P.; Almdal, K.; Mortensen, K.; Fredrickson, G. H. *J. Chem. Phys.* **1988**, *108*, 1989.

MA9918755